AD-A083 796 NORTHWESTERN UNIV EVANSTON IL DEPT OF MATERIALS SCIENCE F/G 14/2
X-RAY TECHNIQUES FOR THE MEASUREMENT OF RESIDUAL STRESSES IN TH--ETC(U)
APR 80 J B COHEN N00014-75-C-0580
UNCLASSIFIED TR-27 NL

END
DATE FILMED
6-80
DTIC

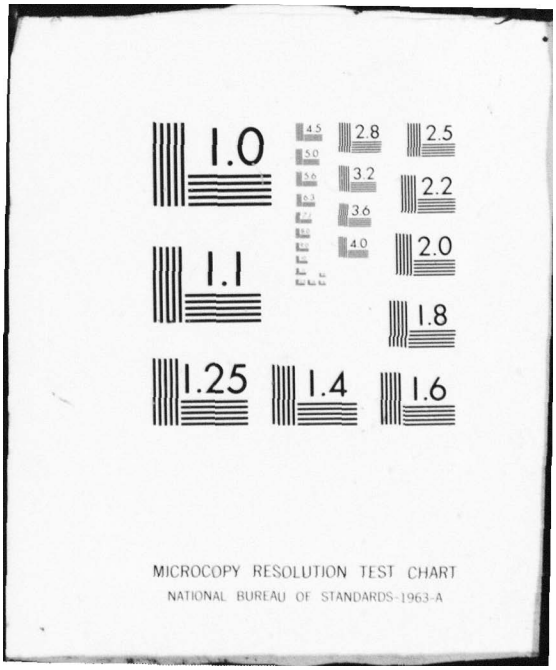
1.0
1.1
1.25
4.5
5.0
5.6
6.3
2.8
3.2
3.6
4.0
2.5
2.2
2.0
1.8
1.4
1.6
MICROCOPY RESOLUTION TEST CHART
NATIONAL BUREAU OF STANDARDS-1963-A

NORTHWESTERN UNIVERSITY

DEPARTMENT OF MATERIALS SCIENCE

Technical Report No. 27
April 8, 1980

Office of Naval Research
Contract N00014-75-C-0580
NR 031-733

X-RAY TECHNIQUES FOR THE MEASUREMENT OF RESIDUAL STRESSES IN THE REAL WORLD

BY

J. B. Cohen

EVANSTON, ILLINOIS

X-RAY TECHNIQUES FOR THE MEASUREMENT OF RESIDUAL STRESSES IN THE REAL WORLD

J. B. Cohen

Dept. of Materials Science & Engineering
the Technological Institute, Northwestern University
Evanston, Illinois 60201

ABSTRACT

The principles of the X-ray method of measuring residual stresses are reviewed, with special emphasis on the latest developments in both procedures and equipment. Rapid in-the-field measurements are now being performed. It is possible to obtain stress gradients without layer removal and to obtain the entire stress tensor (not just the surface stresses).

INTRODUCTION

The x-ray method of measuring stresses is nondestructive and, after half a century of use, it is the standard to which other techniques must be compared. According to Bragg's law, if incident X-radiation of wavelength, λ, strikes a polycrystalline specimen at an angle, θ, grains with interplanar spacing "d" diffract intensity at the same angle, following the equation, $\lambda = 2d \sin\theta$. In Fig. 1a, such a situation is illustrated, with the surface in compression.

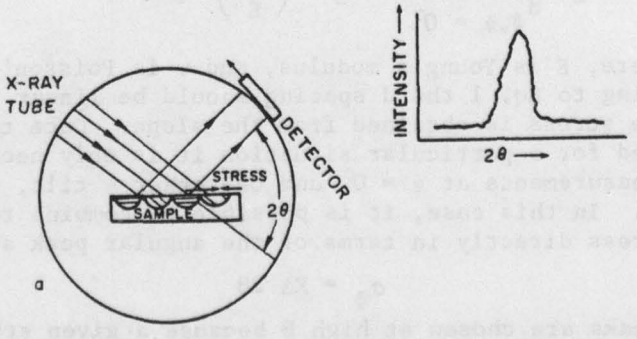

Figure 1 (a) — Schematic of a diffractometer. The incident beam diffracts x-rays of wavelength λ from planes that satisfy Bragg's law in crystals with these planes parallel to the sample's surface. If the surface is in compression, because of Poisson's ratio these planes are further apart than in the stress-free state. The d spacing is obtained from the peak in intensity versus scattering angle 2θ and Bragg's law, λ = 2 d sin θ.

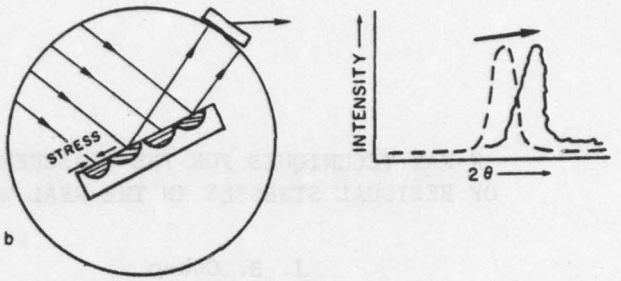

Figure 1 (b) — After the specimen is tilted, diffraction occurs from other grains, but from the same planes, and these are more nearly perpendicular to the stress. These planes are less separated than in (a). The peak occurs at higher angles of 2θ.

Note that only certain grains are oriented to diffract, those with planes of spacing "d" parallel to the surface. Because of Poisson's effect, these planes are dilated by the surface stress and the angle of diffraction is lower than without stress. In Fig. 1b, the sample has been tilted (or the x-ray beam is tilted with respect to the sample). Different grains are diffracting; as these are oriented differently with respect to the stress than in Fig. 1a, the change in d spacing and θ are different. It is these angular shifts due to the change in d spacing that allow us to measure the strain due a residual stress. Only measurements at different tilts are required and it is <u>not</u> necessary to know the value of the d spacing in the unstressed material. Assuming that the measurement samples only the surface (so that there are no stress components normal to the surface) and isotropic elastic theory, the stress at an angle Φ to the principal stresses, is (1):

$$\left[\frac{d_{\Phi,\psi} - d_{\psi,\psi = 0^\circ}}{d_{\Phi,\psi = 0^\circ}}\right] = \left(\frac{1+\nu}{E}\right)\sigma_\Phi \sin^2\psi \ . \qquad (1)$$

Here, E is Young's modulus, and ν is Poisson's ratio. According to Eq. 1 the d spacing should be linear with $\sin^2\psi$ and the stress is obtained from the slope. Once this has been verified for a particular situation it is only necessary to make measurements at $\psi = 0^\circ$ and one other ψ tilt, usually 45° or 60°. In this case, it is possible to combine terms to write the stress directly in terms of the angular peak shift:

$$\sigma_\Phi = K\Delta\ 2\theta \qquad (2)$$

Peaks are chosen at high θ because a given strain, Δd/d, causes the largest angular shift in such a region. It is easy to measure a shift to $\pm .01^\circ\theta$. For steel and $\psi = 45^\circ$, this uncertainty in peak shift is only an uncertainty in stress of ± 12MPa(±1.7KSi), using CrKα radiation and the 211 peak at $\theta = 78^\circ$.

TECHNIQUES

In this brief review, an update on the latest techniques and developments will be stressed. Because of the assumptions made in the derivations of Eq. 1, for accuracy it is best to measure the elastic constant terms by loading the same material elastically to known stress levels and measuring the shift. It is to be emphasized that this is required only for accuracy. If interest lies only in relative values, sufficiently adequate constants are available in the literature or can be easily calculated (2).

In a laboratory such measurements are generally performed on a standard diffractometer. With the advent of mini and micro computers, automation (including sample alignment) has been developed so that it is possible to measure to an operator desired precision, and to calculate the principle errors (3). In fact laboratories with such automation have shown that multiple ψ tilts can be performed in the same total time as a two-tilt procedure with the same or better precision (3).

In view of this, it is strongly recommended that the $\sin^2\psi$ method be adopted in the U.S. when measurements are performed on a diffractometer - as has been done in Japan and Europe.

It is also common in the U.S. to use a three-point parabolic fit to define the peak position. Much improved reproductibility can be obtained with 7 or more points, and this practice should also be adopted (3).

When the $\sin^2\psi$ method is employed, occasionally, large oscillations occur in "d" vs $\sin^2\psi$. This is due largely to elastic anisotropy, and somewhat to plastic anisotropy. After all, different grains are sampled at each ψ tilt. It is in just such situations that quite erroneous results can be obtained with the simple two-tilt procedure. It has now been shown that if hoo or hhh reflections are employed for cubic alloys and ooh reflections are employed with hexagonal materials such oscillations are minimized (4).

To increase the number of grains irradiated, a devergent x-ray beam is generally employed in the U.S. as shown in Fig. 2.

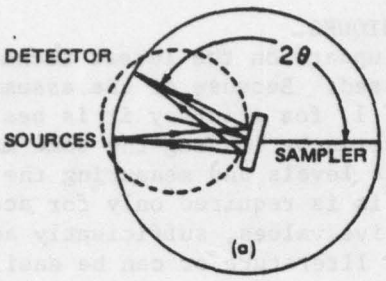

Figure 2 (a) — The divergent beam usually employed on a diffractometer to expose a wide area on the specimen and still have a sharply focused beam at (D). The source (S), sample, and detector (D) are on a circle (shown dotted) to obtain this focusing.

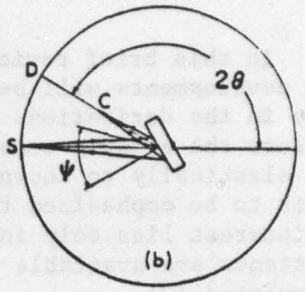

Figure 2 (b) — When the specimen is tilted ψ deg during a stress measurement the focal point shifts to (C). In the parafocusing method the counter is moved to this new position. In the stationary slit method the detector remains at D.

Unfortunately (as shown in this figure) on tilting the specimen the correct geometric focus moves, and it is common practice to move the receiving slits to the new focus to record the sharpest possible peak. This procedure has at least two unfortunate consequences. In the first place, the results become quite sensitive to positioning the sample at the center of the diffractometer. Secondly, when a material has a texture, the motion results in the slit seeing a different fraction of the Debye - Scherrer cone, and hence emphasizing different grains. A vertical slit must be positioned at the detector and not moved with the receiving slit.

Less sensitivity to sample position can be achieved by not moving the slit at all (3). In such a case a correction is needed to the peak position but only if it is very sharp and changes shape with ψ. This correction is readily calculated (5). As an alternative the parallel beam procedure devised in Japan (6) is illustrated in Fig. 3.

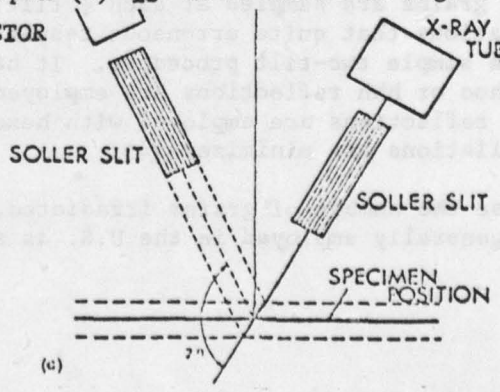

Figure 3 - Parallel beam geometry. The angle 2θ is defined by the angle between two "Soller" slits (which makes the x-ray beam parallel) and is independent of sample position.

Sensitivity to sample position is eliminated (3). This can be achieved with a pinhole beam, or by simply turning the divergent and receiving Soller slits on a diffractometer 90°. The peak is broadened and this increases the measurement time for a given precision (3), but is very worthwhile when sample positioning is difficult, as is often the case. Another procedure is to tilt around an axis parallel to the diffractometer (7), as shown in Fig. 4. No slit motion is required, the absorption correction needed with the other ψ tilt (2) is eliminated, and occasionally this procedure helps in reaching difficult locations.

There are new position sensitive detectors available commercially that record an angular range of 5-10° in θ all at once. With such a detector mounted on a diffractometer, and a multi-channel analyzer, stress measurements can be re-

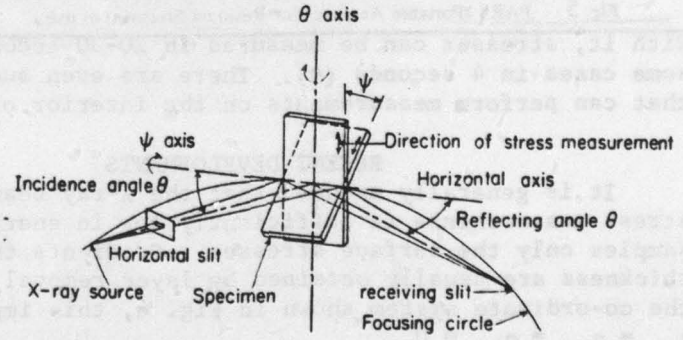

Fig. 4 The ψ diffractometer. Note that the ψ tilt is around an axis in the plane defined by the incident and scattered x-ray beams.

duced in time by a factor of 3-5 (8). Also, because of the wide angular range more than one peak can be recorded and the same instrument can be employed for rapid measurements of retained austenite.

Portable units for field use are now available commercially in various forms, ranging from essentially large diffractometers on wheels, to light hand-held units employing position sensitive detectors and small air-cooled X-ray tubes. An example of the latter is shown in Fig. 5.

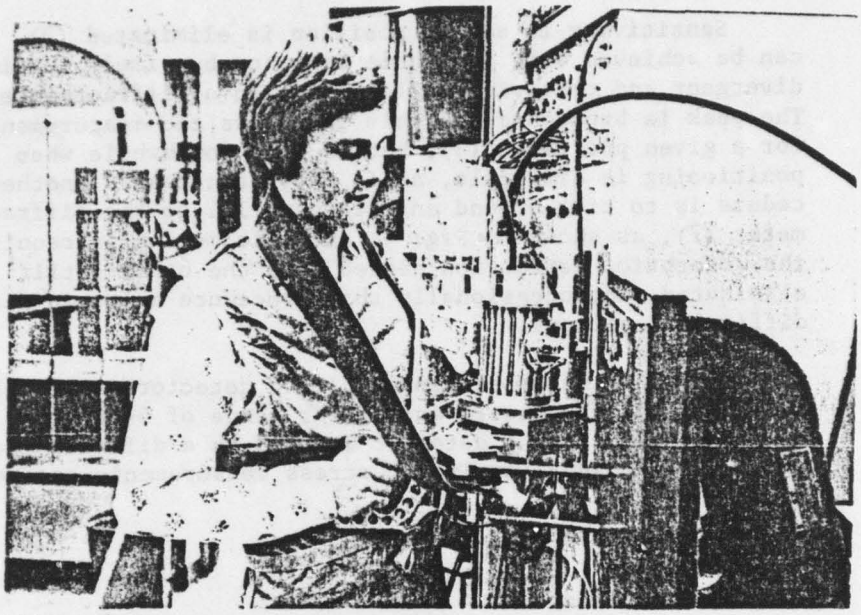

Fig. 5 PARS (Portable Analyzer for Residual Stresses) in use.

With it, stresses can be measured in 20-30 seconds, and, in some cases in 4 seconds (9). There are even such devices that can perform measurements on the interior of pipes (10).

RECENT DEVELOPMENTS

It is generally assumed that the X-ray beam employed in stress measurements is sufficiently low in energy that it samples only the surface stresses. Gradients through the thickness are usually obtained by layer removal (2). With the co-ordinate system shown in Fig. 6, this implies that $\sigma_{33} = \sigma_{13} = \sigma_{23} = 0$.

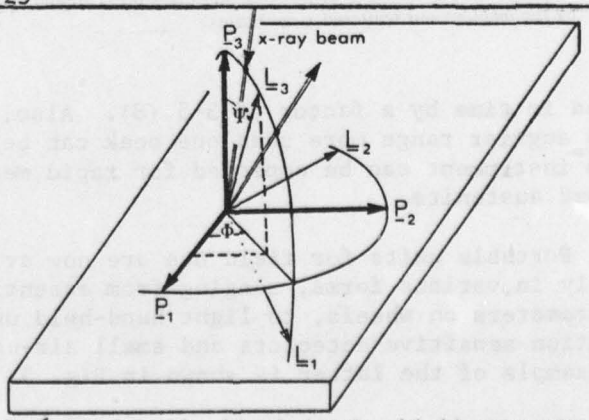

Fig. 6 -Definition of Φ and ψ and orientation of the laboratory system L_i with respect to the sample system P_i. A positive ψ tilt is shown.

With gradients of 15MPa/μm (2Ksi/μm) or more, the presence of such gradients can be detected, because they lead to a gradual curvature in "d" vs $\sin^2\psi$. This is because the depth of x-ray penetration varies with the ψ tilt. Some information on the gradient can be obtained from this curvature without layer removal (5). Assume that:

a) The X-ray elastic constants do not vary with depth,
b) $\Phi = 0^\circ$ (measurements are in the direction of σ_{11}),
c) $\sigma_{11} = \sigma_{22}$ at all depths,
d) $\sigma_{ij}(Z) = 0$ for $i \neq j$ (i.e. there are no shear stresses).

Then:

$$\frac{d_{\Phi,\psi=0} - d_o}{d_o} = \frac{2\nu}{E}\langle\sigma_{11}\rangle + \langle\sigma_{33}\rangle\left[\frac{1+2\nu}{E}\right] . \qquad (3)$$

The brackets imply an average over the depth of penetration of the X-ray beam. Note that in this procedure a value from the literature for the unstressed d spacing is required. Furthermore:

$$\left(\frac{\partial\left(\frac{\Delta d}{d}\right)}{\partial \sin^2\psi}\right)_{\Phi=0} = \frac{1+\nu}{E}\left[\langle\sigma_{11}\rangle - \langle\sigma_{33}\rangle\right] . \qquad (4)$$

By fitting a straight line to the data, first estimates for $\langle\sigma_{11}\rangle$ and $\langle\sigma_{33}\rangle$ can be obtained from Eqn's 3 and 4. From the shape of the actual curve, the sign of the gradient is directly available. For example, if $\sigma_{33}>0$, and the stress increases with depth, d decreases with $\sin^2\psi$ and d vs $\sin^2\psi$ is convex to the $\sin^2\psi$ axis. But if the stress decreases with depth it is concave (5). Some gradient is then assumed, perhaps such as that in Fig. 7. Then the depth Z_2 and the gradient σ_{33} are varied until a match is obtained to:

$$\langle\sigma_{ij}\rangle = \sigma_{ij}(Z=0) + \int_0^D \exp(-Z/\tau)\sigma_{ij}(Z)dZ, \qquad (5)$$

and to the actual slope of d vs $\sin^2\psi$ at various ψ values, Eq. 4. In Eqn. (5), τ is related to the linear x-ray absorption coefficient, μ, and for ψ tilts around the θ axis:

$$\tau = \frac{\sin^2\theta - \sin^2\psi}{2\mu \sin\theta\cos\psi} . \qquad (6)$$

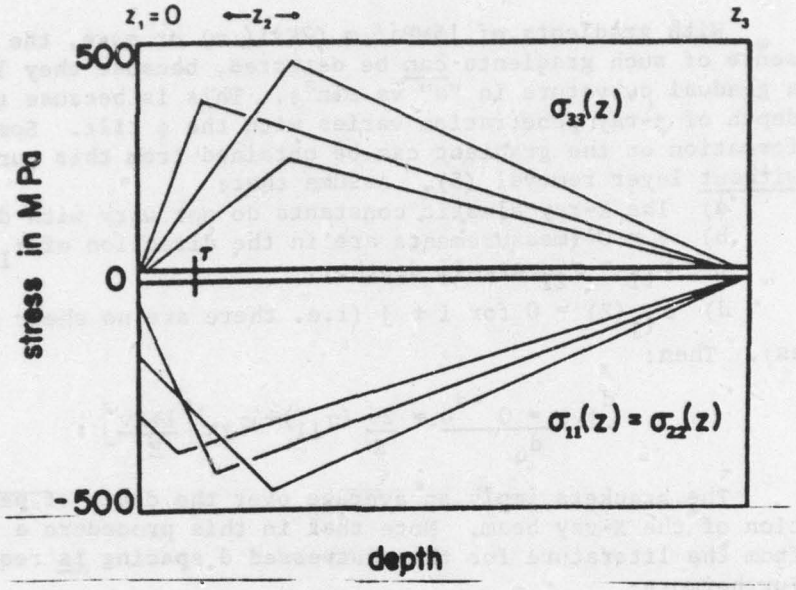

Fig. 7 Assumed gradients

This procedure could be particularly fruitful when many similar samples have to be examined for their gradients, and the general shape of the gradient is known from one experiment involving layer removal. An example of such work is given in ref. 5.

In the presence of such strong gradients it is also possible to detect shear components. Again, employing the co-ordinate system in Fig. 6 and with a prime implying a measurement in the axial system L_i, unprimed quantities in the axial system, P_i, (11):

$$\langle \varepsilon'_{33} \rangle = \frac{d_{\Phi,\psi} - d_o}{d_o} = \langle \varepsilon_{11} \rangle \cos^2\Phi \sin^2\psi + \langle \varepsilon_{12} \rangle \sin 2\Phi \sin^2\psi + \langle \varepsilon_{13} \rangle \cos\Phi \sin 2\psi$$

$$+ \langle \varepsilon_{22} \rangle \sin^2\Phi \sin^2\psi + \varepsilon_{23} \sin\Phi \sin 2\psi + \varepsilon_{33} \cos^2\psi \ . \qquad (7)$$

There are terms in this equation which depend on $\sin 2\psi$, not $\sin^2\psi$, and therefore "d" vs $\sin^2\psi$ will be different for $\pm\psi$, as can be seen in Fig. 8. It is this difference in the plot for $\pm\psi$ that distinguishes the presence of ε_{23}, ε_{13} from effects due to gradients in the normal stress components, or those due to anisotropic elasticity. (If tilts in both ψ directions are difficult, it is only necessary to rotate the specimen 180° around its normal and repeat the measurement of d vs $\sin^2\psi$.)

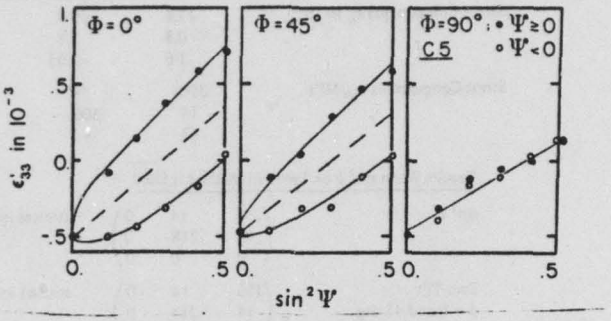

Fig. 8 - Lattice strain vs. $\sin^2\psi$ for various directions on the surface (Φ), and $\pm\psi$ tilts. Ground soft steel. (From reference 12.)

Defining $a_1 = \frac{1}{2}\left[\epsilon_{\Phi\psi+} + \epsilon_{\Phi\psi-}\right]$ and a_2 as $\frac{1}{2}\left[\epsilon_{\Phi\psi+} - \epsilon_{\Phi\psi-}\right]$, then:

$$a_1 = \langle\epsilon_{33}\rangle + \left[\langle\epsilon_{11}\rangle\cos^2\Phi + \langle\epsilon_{12}\rangle\sin 2\Phi + \langle\epsilon_{22}\rangle\sin^2\Phi - \langle\epsilon_{33}\rangle\right]\sin^2\psi, \quad (8)$$

$$a_2 = \left[\langle\epsilon_{13}\rangle\cos\Phi + \langle\epsilon_{23}\rangle\sin\Phi\right]\sin|2\psi| \ . \quad (9)$$

Thus $\langle\epsilon_{33}\rangle$ is obtained from the intercept of a_1 vs $\sin^2\psi$. At $\Phi = 0^\circ$, $\partial a_1/\partial\sin^2\psi$ gives $\langle\epsilon_{11}\rangle - \langle\epsilon_{33}\rangle$ and hence $\langle\epsilon_{11}\rangle$, whereas at $\Phi = 90^\circ$ $\langle\epsilon_{22}\rangle$ is obtained. The ϵ_{12} component is then determined from $\frac{\partial a_1}{\partial \sin^2\psi}$ at $\Phi = 45^\circ$. From $\frac{\partial a_2}{\partial \sin|2\psi|}$, ϵ_{13} is calculated for $\Phi = 0^\circ$, ϵ_{23} for $\Phi = 90^\circ$. The curves in Fig. 8, are Eqn. 7 with the values from this procedure. The stresses can then be obtained from:

$$\sigma_{ij} = \frac{E}{1+\nu}\left[\epsilon_{ij} - \delta_{ij}\frac{\nu}{1+2\nu}(\epsilon_{11} + \epsilon_{22} + \epsilon_{33})\right], \quad (10)$$

where $\delta_{ij} = 0$ for $i \pm j$.

Shear stresses can arise on worn surfaces, or after rolling or grinding. An example of the results from a recent study of grinding of steel (12) is given in Fig. 9. Note particularly how much error is made if these shear components are neglected in a "normal" stress measurement.

Fig. 9 .. Experimental Results for Specimen C5 (Fig. 8)

Strain Components ϵ_{ij} in 10^{-4}	12.6	0.8	3.6
	0.8	7.8	-0.05
	3.6	-0.05	-4.5
Stress Components σ_{ij}, MPa	390	14	63
	14	306	-1
	63	-1	92

Results When $\sin^2\psi$ or Two-Tilt Method is Used

$\sin^2\psi$	$\begin{pmatrix} 298 & 14 & 0 \\ 14 & 218 & 0 \\ 0 & 0 & 0 \end{pmatrix}$	stresses in MPa
Two-Tilt ψ = 0 and 45 deg	$\begin{pmatrix} 356 & 14 & 0 \\ 14 & 218 & 0 \\ 0 & 0 & 0 \end{pmatrix}$	stresses in MPa
Two-Tilt ψ = 0 and -45 deg	$\begin{pmatrix} 151 & 14 & 0 \\ 14 & 218 & 0 \\ 0 & 0 & 0 \end{pmatrix}$	stresses in MPa

CONCLUDING REMARKS

The X-ray measurement of residual stresses is a well established technique ready to use in the field. However, it is worth pointing out that X-rays measure all the stresses - those produced because of differences in deformation of various parts of a body (the so-called macrostresses) and those that arise due to stress concentrations from second phases, or grain junctions, from one grain acting on another, or due to different dislocation densities inside a subgrain and at the subgrain wall. Some other procedures, such as disection, measure only macrostresses. But since failures start locally, the total stress is probably of most concern.

ACKNOWLEDGEMENT

The author would like to thank ONR for its support in this area over the past decade, particularly Dr. B. McDonald.

REFERENCES

(1) B. D. Cullity "Elements of X-ray Diffraction", 2nd ed. Addison, Wesley, Reading, Mass. 1978, Ch. 16, pp. 447-479.

(2) Society of Automotive Engineers, SAE Handbook Supplement J784a "Residual Stress Measurement by X-ray Diffraction", SAE, Inc. New York, 1971.

(3) M. R. James and J. B. Cohen, "Study of the Precision of X-ray Stress Analysis", Adv. in X-ray Analysis, 20, 1977, pp. 291-307.

(4) H. Dölle and J. B. Cohen "Evaluation of Stresses in Textured Cubic Metals", Met. Trans. in Press.

(5) J. B. Cohen, H. Dölle and M. R. James, "Stress Analysis from Powder Diffraction Patterns", NBS Conference on Accuracy in Powder Diffraction, in Press.
(6) The Society of Materials Science, Japan "Standard Method for X-ray Stress Measurement", 1973. Supplement VI (K. Hayashi).
(7) E. Macherauch and U. Wolfstieg, "A Modified Diffractometer for X-ray Stress Measurements", Adv. in X-ray Analysis, 20, 1977 pp. 369-377.
(8) M. R. James and J. B. Cohen, "The Application of a Position-Sensitive X-ray Detector to the Measurement of Residual Stresses", Adv. in X-ray Analysis, 19, 1976, pp. 695-708.
(9) M. R. James and J. B. Cohen, "PARS - A Portable X-ray Analyzer for Residual Stresses", J. Testing and Evaluation 6, 1978, pp. 91-97.
(10) C. O. Ruud "X-ray Analysis and Advances in Portable Field Instrumentation", J. Metals, June 1979, pp. 10-15.
(11) H. Dölle, "Influence of Multiaxial Stress States, Stress Gradients and Elastic Anisotropy on the Evaluation of Stress by X-rays", J. Appl. Cryst., 12, 1979, pp. 489-501.
(12) H. Dölle and J. B. Cohen, "Residual Stresses in Ground Steels", Met. Trans. 11A, 1980, pp. 159-164.

Unclassified

Security Classification

AD-A083796

DOCUMENT CONTROL DATA - R & D

(Security classification of title, body of abstract and indexing annotation must be entered when the overall report is classified)

1. ORIGINATING ACTIVITY *(Corporate author)*

J. B. Cohen
Northwestern University
Evanston, Illinois 60201

2a. REPORT SECURITY CLASSIFICATION

Unclassified

2b. GROUP

3. REPORT TITLE

(6) X-RAY TECHNIQUES FOR THE MEASUREMENT OF RESIDUAL STRESSES IN THE REAL WORLD.

4. DESCRIPTIVE NOTES *(Type of report and inclusive dates)*

Technical Report No. 27

5. AUTHOR(S) *(First name, middle initial, last name)*

(10) Jerome B. Cohen

(12) 14

6. REPORT DATE

(11) Apr[illegible] 1980

7a. TOTAL NO. OF PAGES

14

7b. NO. OF REFS

12

8a. CONTRACT OR GRANT NO.

(15) N00014-75-C-0580

b. PROJECT NO.

NR 031-733, Mod. No. P00005

c.

d.

9a. ORIGINATOR'S REPORT NUMBER(S)

27

9b. OTHER REPORT NO(S) *(Any other numbers that may be assigned this report)*

10. DISTRIBUTION STATEMENT

Distribution of this document is unlimited

(14) TR-27

11. SUPPLEMENTARY NOTES

12. SPONSORING MILITARY ACTIVITY

Metallurgy Branch
Office of Naval Research

13. ABSTRACT

The principles of the X-ray method of measuring residual stresses are reviewed, with special emphasis on the latest developments in both procedures and equipment. Rapid in-the-field measurements are now being performed. It is possible to obtain stress gradients without layer removal and to obtain the entire stress tensor (not just the surface stresses).

(9) Technical rept.,

260810

DD FORM 1 NOV 65 1473 (PAGE 1)

S/N 0101-807-6801

Unclassified

Security Classification

14. KEY WORDS	LINK A		LINK B		LINK C	
	ROLE	WT	ROLE	WT	ROLE	WT
residual stresses, x-ray measurement of stresses						